Journal of Materials Chemistry C

PAPER

View Article Online
View Journal | View Issue

Cite this: *J. Mater. Chem. C*, 2018, **6**, 1048

Kinetically controlled synthesis of Cu nanowires with tunable diameters and their applications in transparent electrodes†

Xiao Wang, Ranran Wang,* Liangjing Shi and Jing Sun *

Received 6th November 2017,
Accepted 20th December 2017

DOI: 10.1039/c7tc05038k

rsc.li/materials-c

One-dimensional metallic nanostructures have attracted ever increasing attention in recent years due to their potential applications in transparent electrodes, catalysts, surface enhanced resonance scattering (SERS) based sensors and electric heating elements. The controllable synthesis of high quality metal nanowires is of great importance for the optimization of devices based on metal nanowires. However, due to the intrinsic complexity of one-pot organic reaction systems, the reaction mechanism is still yet to be understood, which severely holds back the efforts towards the controllable synthesis of high quality nanowires. Herein, a two-step method for the synthesis of high-quality Cu nanowires with tunable diameters is proposed. The mechanism of a typical synthesis procedure is discussed through analyzing the apparent phenomena and intermediate products. Kinetically controlled synthesis is achieved by adjusting the species and concentration of halide ions to synthesize high-purity Cu nanowires with tunable diameters ranging from 20 to 90 nm. Electrodes with superior conductivity (FoM ~ 140, 11 Ω sq^{-1}@80%) are constructed and characterized on the basis of the Cu nanowires synthesized through this method. Red shifts in the LSPR peaks of Cu nanowire dispersions and increments in the haze factors of nanowire electrodes are observed as the average diameter of Cu nanowires increases. The method is also successfully expanded to the synthesis of Ag nanowires with tunable diameters.

Introduction

One-dimensional metallic nanostructures have attracted ever increasing attention in recent years. Due to their high conductivity, flexibility, low cost and easy accessibility, one-dimensional metal nanostructures have been regarded as ideal building blocks for various electronic and electro-chemical devices.[1–3] As such, many efforts have been made for the synthesis of high-quality metal nanowires. Thanks to these efforts, Cu nanowires, Ag nanowires, Ni nanowires and various bimetal nanowires have been developed.[4] The superior intrinsic conductivity, high electron density and outstanding optical scattering ability have attracted a lot of research interest for Ag nanowires. Ag nanowires have been successfully used in constructing high-performance devices such as flexible conductors[5] and solar cells.[3,6] However, the high cost of silver severely limits the commercial applications of Ag nanowires. Cu nanowires also have excellent intrinsic conductivity (second only to silver), abundant supply (1000 times more than silver)[2] and easy accessibility, which makes them preeminent candidates for high performance devices.[2,7,8]

The last decade has witnessed substantial progress in the synthesis of one-dimensional Cu nanostructures. Cu nanowires with an average diameter of 78 nm were synthesized using a self-catalytic method within a liquid-crystalline medium composed of hexadecylamine (HDA) and cetyltriammonium bromide (CTAB).[2] Jin *et al.* synthesized Cu nanowires with an average diameter of 24 nm *via* an aqueous system with glucose as the reducing agent and HDA as the capping agent.[7] Cu nanowires with an even smaller average diameter of 16 nm were synthesized by Peng *et al.* through a solvothermal method, in which OLA was used as the reducing agent and solvent.[9] However, despite all those achievements in synthesizing high-quality Cu nanowires, the problems of concomitant nanoparticles, high diameter dispersity of nanowires and controllable synthesis of Cu nanowires with tunable diameters are yet to be solved.

The performance of metal nanowire-based devices has been established to be strongly dependent on their purity (the amount of unwanted nanoparticles or other low-aspect-ratio geometries) and dimensions.[10] The existence of concomitant

State Key Laboratory of High Performance Ceramics and Superfine Microstructure, Shanghai Institute of Ceramics, Chinese Academy of Sciences, China.
E-mail: wangranran@mail.sic.ac.cn, jingsun@mail.sic.ac.cn

† Electronic supplementary information (ESI) available: Photos of reaction systems at different stages; the EDS spectrum of the intermediate product separated at the end of Stage I of a typical procedure; photos of reaction systems 5 min after the addition of CuX_2; HRTEM images and SAED patterns of the as synthesized Cu nanowires; SEM images of Ag nanowires synthesized under different conditions. See DOI: 10.1039/c7tc05038k

nanoparticles and the high diameter dispersity of nanowires synthesized through chemical methods may severely detriment the performance of metal nanowire based devices.[11] They do not only bring difficulties into the subsequent material processing steps and degrade the performance of devices, but also hinder the efforts towards the systematically experimental evaluation of nanowires with different diameters.[11] The demand for high-performance transparent electrodes creates an urge for the controllable synthesis of high quality Cu nanowires. Besides, metal nanowires with different ranges of diameters have different optical and electrical performances and are usually suitable for different applications.[12,13] The purposive arrangement of nanowires with different diameters would also benefit the fabrication of high-performance devices. The demand for metal nanowires with monodisperse and tunable diameters stimulates the development and optimization of new synthesis methods.

As reported previously, a typical synthesis procedure of metal nanostructures could be divided into three stages: the formation of nuclei, the evolution from nuclei to seeds and the growth from seeds to nanocrystals.[14] The geometry of as synthesized nanowires is mainly determined by the size of seeds formed in the nuclei to the evolution process of seeds and the anisotropic growth of one-dimensional nanostructures, both of which could be influenced by the reduction kinetics. The control over reduction kinetics provides us with a potential way in achieving high-quality Cu nanowires with tunable diameters. However, it remains a grand challenge to realize the effective control over the reduction rates. This challenge could be attributed to the following possible reasons: (i) for a one-pot method which is widely used in current synthesis processes, the fact that multiple reactions occur simultaneously holds back the effort towards understanding the evolution process of Cu nanowires. (ii) The spontaneous nucleation process causes particles to grow through multiple pathways, which leads to the formation of unwanted shapes. (iii) The reaction kinetics could be influenced by many factors such as the concentration of free metal ions and the oxidative etching process. The adjustment of any single parameter may show synergistic or contradictory effects on these factors, which makes it difficult to distinguish the key parameter that determines the morphology of nanowires.

As the geometry of nanowires might be influenced by the reaction kinetics of every stage, the understanding of the reaction mechanism of each stage and distinguishing the key parameters that influence the reaction kinetics are essential. In order to overcome the aforementioned difficulties, we proposed a two-step method through which high-quality Cu nanowires could be achieved. Pre-formed nucleation centers were introduced by separating the birth of nucleation centers and the formation of nanoseeds to ensure the even formation of seeds, and thus led to nanoseeds similar in size and structure. Halide ions were found to play an important role in determining the degree of oxidative etching and the concentration of free ions. Besides, the preferential adsorption of halide ions on the {111} facets could also initiate the anisotropic growth of Cu nanowires. The adjustment of halide ions has not only provided us with an efficient way in controlling reduction kinetics and achieving a kinetically controlled synthesis, which is essential to the synthesis of high quality Cu nanowires, but also enabled the synthesis of Cu nanowires with tunable diameters. By adjusting the concentration and species of halide ions, both the size of nanoseeds and the population of nanoseeds with different structures were well controlled. High purity Cu nanowires with variable average diameters ranging from 20 to 90 nm were synthesized. This approach could also be applied to the synthesis of other one-dimensional metal nanostructures such as Ag nanowires. On the basis of the Cu nanowires synthesized using this method, the optical and electrical properties of the electrodes composed of Cu nanowires were characterized to understand the influences of the diameters of nanowires. As the average diameters of Cu nanowires increased from 20 to 90 nm, a red shift in the LSPR peaks of Cu nanowire dispersions and an increase in the haze factors of nanowire electrodes were observed.

Experimental section

Materials

Cupric(II) acetylacetonate ($Cu(acac)_2$, 99%), copper chloride ($CuCl_2$, 99%), nickel(II) 2,4-pentanedionate ($Ni(acac)_2$, 95%), oleylamine (OLA, 80–90%), nickel chloride hexahydrate ($NiCl_2 \cdot 6H_2O$, 98%), copper(II) bromide ($CuBr_2$, 98.5–100.5%), silver nitrate ($AgNO_3$, 99.8%), and silver bromide (AgBr, 99.5%).

Synthesis of Cu nanowires

In a typical synthesis procedure, a copper precursor ($Cu(acac)_2$), $Ni(acac)_2$ and oleylamine were mixed and stirred at 80 °C to form a uniform light blue solution. The solution was then aged at an increased temperature of 165 °C for 55 min. A mixture of $CuCl_2$ and oleylamine was added to the solution. Cu nanowires could be obtained after 4 hours of reaction. The whole reaction process was protected by a flow of argon. $NiCl_2$ was used to adjust the concentration of Cl^- without influencing the concentration of Cu(II) ions.

Synthesis of Ag nanowires

Ag nanowires were synthesized using a similar method to the one used for the synthesis of Cu nanowires. The Ag precursor ($AgNO_3$), $CuBr_2$ and oleylamine were mixed and stirred at 80 °C for 40 min to ensure the complete resolution of metal salts. The temperature was then increased to 125 °C to initialize the reduction of Ag^+ ions. After being incubated at 125 °C for 4 h with the protection of argon flow, Ag nanowires could be obtained from the reaction system.

Characterization

The micro-morphology characterization was carried out using a field emission scanning electron microscope (SEM, HITACHI UHR FE-SEM SU 8220) at an accelerated voltage of 3.0 kV. A transmittance electron microscope (TEM, JEOL JEM-2100F) was used to provide information on the micro-morphology as well as interior structures of the reaction products. XRD analysis was carried out on an X-ray diffractometer (Rigaku D/max 2550V).

Results and discussion

The synthesis of Cu nanowires

In a typical synthesis procedure, oleylamine was used as the solvent and the reducing agent, while $Cu(acac)_2$ was used as the copper precursor. $Ni(acac)_2$ was added to accelerate the reduction of Cu ions. Based on the operation steps and the experimental phenomena observed, the synthesis process was divided into three stages: the birth of nucleation centers, the formation of seeds and the anisotropic growth of Cu nanowires.

The birth of nucleation centers

During the first stage, which was defined as the birth of nucleation centers, $Cu(acac)_2$, $Ni(acac)_2$ and oleylamine were mixed and stirred at 80 °C to form a uniform light-blue solution. The temperature was then increased to 165 °C to enable the reduction of Cu ions and the formation of Cu nanoparticles. After being aged at 165 °C for 55 min, a copper mirror could be observed on the wall of the reaction vessel, bespeaking the formation of Cu nanoparticles (Fig. S1a, ESI†). Products of this stage were separated and characterized through TEM and HRTEM. As shown in Fig. 1, nanoparticles with an average diameter of 18 nm were synthesized during Stage I. Both single crystals and twinned nanoparticles with similar diameters could be observed in the high-resolution TEM (HRTEM) image (Fig. 1b). The EDS of the nanoparticles showed that in addition to copper, nickel also existed in the nanoparticles, indicating that a co-reduction mode exists in the formation of Cu nanoparticles (Fig. S2, ESI†). As reported previously, this co-reduction mode could effectively accelerate the reduction of Cu ions.[9] Due to the heterogeneous nucleation effect, Cu nanoparticles preferentially generated on the wall of the reaction vessel and formed the copper mirror observed at the end of Stage I (Fig. S1, ESI†).

The etching of nanoparticles and the formation of seeds

Unlike the one-pot method reported previously, the birth of nucleation centers and the evolution from nanoparticles to seeds were separated to obtain a clear image. After the formation of Cu nanoparticles, a mixture of $CuCl_2$ and oleylamine was added to the reaction system using a syringe. After the injection, the reaction system gradually turned clear together with the disappearance of the copper mirror within 5 minutes. The formation of a clear solution with a color of orange has long been suspected as a result of the coordination between OLA and Cu(II). This possibility was examined through replacing $CuCl_2$ with $Cu(acac)_2$ in Stage II of a conventional reaction procedure. After the addition of $Cu(acac)_2$, incomplete disappearance of the copper mirror was observed, indicating the importance of Cu(II) ions in the etching process. However, unlike the reaction systems based on $CuCl_2$, neither a color change nor a clear solution could be observed, showing that Cl^- ions had a promoting effect in the etching of pre-formed Cu nanoparticles. We therefore attributed the alternation of the reaction system from a solution of marazine-blue color and a copper mirror to a clear solution of orange color to the oxidative etching of pre-formed nanoparticles caused by the addition of Cu(II) and Cl^-. After being added to the reaction system, Cu(II) ions would soon etch the pre-formed Cu nanoparticles into Cu(I) ions through a comproportionation reaction. The coordination between Cu(I) ions and Cl^- further prompted the reaction (eqn (1)). Unlike the oxidative etching involving reaction systems reported previously, this present reaction system exhibited few differences with or without the protection of Argon gas flow, indicating that instead of Cl^- and oxygen, which were reported to be the oxidative etching pair,[15] the oxidation etching pair here was composed of Cl^- and Cu(II) ions (eqn (1)). According to the wet etching model, Cl^- here played an important role as the coordination ligand in the oxidative dissolution process[14] while Cu^{2+} acted as the

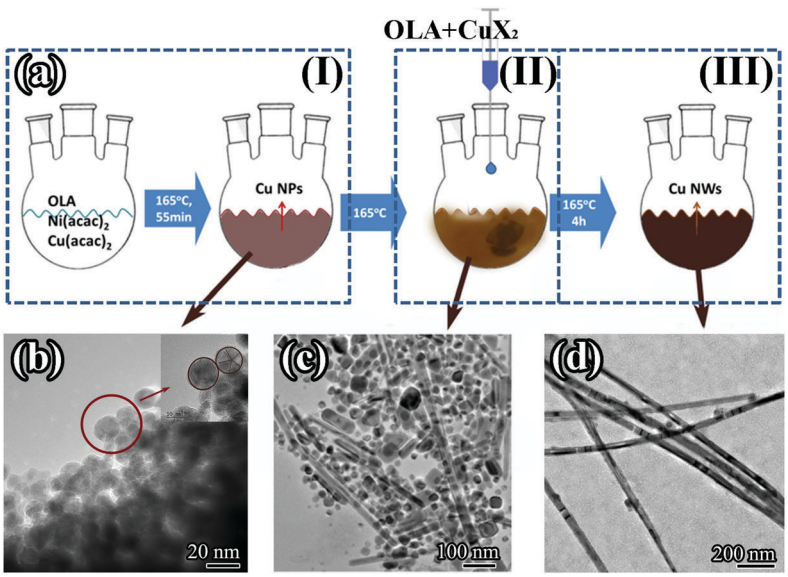

Fig. 1 The schematic illustration of a typical synthesis procedure and the micro-morphologies of the intermediate products of every stage.

oxidizer. As the stability constant of the Cu(I) ion-Cl^- coordination compound (5.5, 25 °C) is much higher than that of the Cu(II) ion-Cl^- coordination compound (0.1, 25 °C), Cl^- would preferentially coordinate with Cu(I) ions, therefore accelerate the etching of Cu nanoparticles. Some Cu nanoparticles survived the etching process and worked as nucleation centers. The introduction of pre-formed nucleation centers enabled the even growth of nanoseeds, and ensured the formation of nanoseeds with similar sizes and structures.

$$Cl^- + Cu^{2+} + Cu \rightarrow [CuCl_x]^{1-x} \quad (1)$$

Considering the importance of halide ions in the oxidative etching of Cu nanoparticles, the etching results and the amount of pre-formed nanoparticles remaining in the reaction system could be influenced by the amount and complex strength of halide ions. Controlled experiments were operated to study the influence of halide ions. With the amount of Cl^- ions decreasing from 2.6 mmol to 2 mmol and 1.6 mmol, the color of the solution gradually turned from orange-yellow to orange-red (Fig. S3, ESI†), indicating that the coordination between Cu^{2+} and Cl^- has a great influence on the concentration of the Cu(I)–Cl^- complex and the amount of reserving pre-formed Cu nanoparticles.[16] To further confirm the speculation, 1.6 mmol Br^- (a weaker coordination compound) was applied to replace Cl^- ions and a clear deep-red solution (more reserving pre-formed Cu nanoparticles) without any precipitation could be observed. The result could be easily understood by the role of halide ions in determining the degree of etching. As shown by eqn (1), changing the coordination ability (from Cl^- to Br^-) or the amount of X^- ions would effectively influence the comproportionation reaction between Cu(II) and Cu, thus affecting the etching of pre-formed Cu nanoparticles. The discrepancies in the amount of reserving pre-formed nanoparticles are the main reasons for the differences in the color of the reaction systems and may further influence the formation of nanoseeds.

The reaction system was then aged at 165 °C for 30 min until the solution turned milky. As it is formidable to determine the formation of nanoseeds, we took the point at which suspended matter started to become visible at the end of the formation of nanoseeds. TEM images of the reaction products 120 min after the addition of $CuCl_2$ and oleylamine indicated the evolution from nanoparticles to seeds (Fig. 2). Nanoseeds and nanorods with comparable average diameters of around 20 nm were observed. Most of the nanoseeds and nanorods possessed five-fold symmetry (Fig. S4, ESI†). Nanoseeds with a square shape were also observed, which were found to be single-crystalline. Given the five-twinned structure of Cu nanowires, the nanoparticles and nanorods with five-fold symmetry tended to be the seeds for nanowires while the single-crystalline nanostructures would grow up into concomitant nanocubes.[13]

For the purpose of obtaining high quality Cu nanowires with less or no concomitant nanoparticles, it is quite important to reduce the number of single-crystalline nanoseeds. The population of nanoseeds with different structures was mainly determined by the statistical thermodynamics of the free energies of different

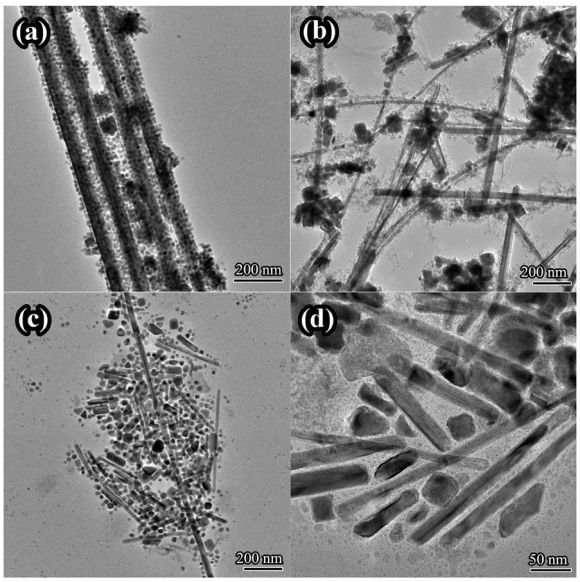

Fig. 2 TEM images of the intermediate products separated at the end of Stage II. (a) 0.8 mmol $CuBr_2$; (b) 0.8 mmol $CuCl_2$; (c) 0.8 mmol $CuCl_2$ and 0.2 mmol $NiCl_2$; (d) 0.8 mmol $CuCl_2$ and 0.5 mmol $NiCl_2$.

species and the kinetic effects regarding the generation and addition of metal atoms to a nucleus.[14] As reported previously, for metal with fcc-structures, only single-crystals and relatively small multiply twinned seeds are favored by thermodynamics.[14] As a result, the formation of seeds must be limited to a kinetically controlled pathway to obtain seeds with a five-fold systematic structure. Practically, the key point of kinetically controlled synthesis is to lower the concentration of metal atoms in solution[14] by regulating the reduction rate of metal ions, which, specific to this present reaction system, could be achieved by adjusting the concentration of free Cu(I) ions. Besides, as the evolution process was carried out on the basis of the reaction solution after etching, the formation of nanoseeds would also be influenced by the etching results. For reaction systems applying 0.8 mmol $CuBr_2$ (1.6 mmol Br^-), red suspension was observed within 10 min after the addition of $CuBr_2$. Nanoseeds (including nanocubes, nanorods and five-twinned nanoseeds) with an average diameter of 56 nm as well as smaller pre-formed nanoparticles with an average diameter of 15 nm coexisted in the intermediate products. However, when 0.8 mmol $CuCl_2$ was added to the solution, the time it took to form a milky solution could be as long as 30 min. TEM images of mid-products separated at the end of the seed formation process showed fewer pre-formed nanoparticles. Nanoseeds with an average diameter of 31 nm were observed. As the amount of Cl^- ions used further increased to 2 mmol and 2.6 mmol, the time needed for precipitation changed to 90 min and 120 min, and the diameter of nanoseeds (nanocubes and 5-twinned nanoseeds) decreased to 26.6 nm and 19 nm, respectively. The uniformity of diameters increased as the amount of Cl^- increased (Fig. 4). As the anisotropic growth of Cu nanowires occurred on these nanoseeds, the high uniformity of nanoseeds would lead to Cu nanowires with uniform diameters. Apart from size, the application of higher

concentration of Cl^- also benefits the generation of nanoseeds with a favored five-fold twinned structure while reducing the number of single-crystalline nanoseeds (Fig. 2d).

The differences were caused by the synergistic effect of two factors. On one hand, for reaction systems with higher concentration of Cl^- ions, a more thorough etching would occur due to the coordination between Cu(I) ions and Cl^- ions and fewer pre-formed Cu nanoparticles would be left. As aforementioned, these Cu nanoparticles could accelerate the reduction of Cu(I) ions and the formation of Cu nanoseeds. A lower concentration of nucleation centers would reduce the reduction rate of Cu ions. The speed of the seed-formation-process slowed down and more time would be needed. On the other hand, the coordination between Cu(I) ions and Cl^- ions would lower the concentration of free Cu(I) ions, which would further slow down the reduction process. Kinetically controlled synthesis would take place in the formation of Cu seeds, in which nanoparticles with lower total free energy are favored.[14] Under this certain circumstance, small five-fold twinned Cu nanoparticles other than single crystals were more likely to form and work as the starting seeds of Cu nanowires.[13] Through adjusting the concentration of halide ions and regulating the degree of oxidative etching in the seed formation stage, a kinetically controlled synthesis process was achieved. Not only the size, but also the population of different seeds could be manipulated effectively, which potentiated the controllable synthesis of high quality Cu nanowires.

The anisotropic growth of Cu nanowires

High quality Cu nanowires were observed at the bottom of the reaction vessel 4 hours after the injection of CuX_2. Fig. 3 shows the SEM and TEM images of Cu nanowires synthesized through a typical procedure. Cu nanowires with a uniform diameter, few unwanted low-aspect-ratio geometries and a smooth surface were observed (Fig. 3a and b). The anisotropic growth of Cu nanostructures occurred during this stage. The XRD spectrum showed a pure nature of the as-synthesized Cu nanowires (Fig. 3b). The HRTEM image of a nanowire showed a clear twinned plane (Fig. 3d). As illustrated by HRTEM images and SAED patterns, five-twinned Cu nanowires with {100} facets as side surfaces and {111} facets bound at the ends were synthesized (Fig. S5, ESI†). Anisotropic growth occurred along the ⟨110⟩ direction.

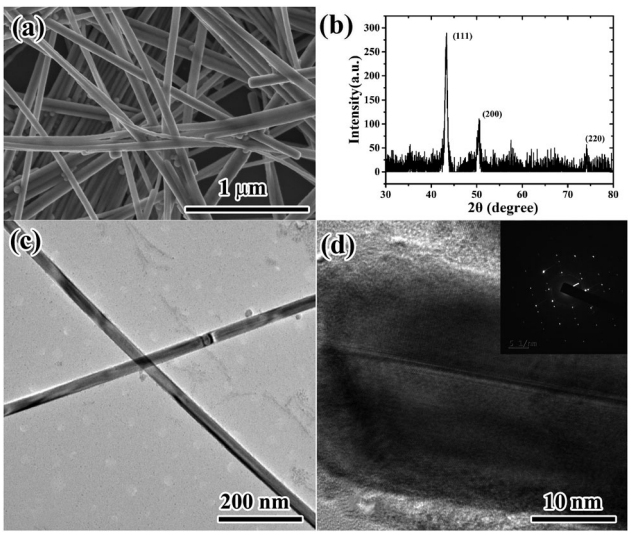

Fig. 3 SEM image (a), XRD spectrum (b), TEM image (c) and HRTEM image (d) of Cu nanowires. The inset of (d) gives the SAED spectrum of a Cu nanowire.

The anisotropic growth of Cu nanostructures has been suspected as a result of the preferential absorption of OLA or other amines and the coordination between Cu ions and amines.[13] However, when $Cu(acac)_2$ was used to replace CuX_2, only Cu nanoparticles were synthesized at the end of the synthesis procedure, revealing the importance of X^- ions and nanoseeds with specific morphologies in the anisotropic growth of Cu nanostructures. Taken together, these observations strongly suggested that apart from OLA (or other amines), the existence of halide ions is also essential for the anisotropic growth of Cu nanostructures and different halide ions may lead to different products.

Given the oleylamine-rich reaction system used in the synthesis of Cu nanowires and the high equilibrium constant of Cu(I) ion-amine coordination compounds, oleylamine will adsorb onto every exposed facet of Cu nanoparticles. However, due to the stereo-hindrance effects, preferential adsorption of oleylamine will occur on {100} facets while Cl^- ions are preferentially adsorbed onto the {111} facets of Cu nanoparticles. Due to coordination between Cl^- and Cu(I) ions, the concentration of Cu(I) ions will be higher around the {111} facets, allowing the preferential deposition of Cu atoms on these facets and thus leading to the anisotropic growth of Cu nanoparticles along the ⟨110⟩ direction. In contrast, oleylamine preferentially absorbed onto the {100} facets also works as the crystal-face-blocking ligand and promotes the anisotropic growth.

Similar to the formation of seeds, the reaction kinetics of the anisotropic growth stage was also influenced by the concentration of halide ions used in the reaction system. For the purpose of discovering the influence of halide ions, we compared the size of nanoseeds with the diameters of nanowires for each specimen. Different trends were observed for reaction systems with different species and amounts of halide ions. For reaction systems using 1.6 mmol Br^- ions or 1.6 mmol Cl^- ions, the average diameters of mid-products (56 nm and 31 nm, respectively) were much smaller than those of the final products (90 nm and 62 nm). Upon increasing the amount of Cl^- ions, the gap between the average diameters of nanoseeds and nanowires tended to decrease. For reaction systems applying 2.0 mmol Cl^- ions and 2.6 mmol Cl^-, the average diameters of mid-products were 26.6 nm and 19 nm, while the average diameters of nanowires synthesized under these conditions were 47 nm and 20 nm. Though similar trends were observed in both seeds and nanowires (the average diameters decreased as the amount of X^- ions increased), the changes of diameters during the growing processes were different for each specimen. As suggested by these results, halide ions played an important role not only in the seeding process, but also in the anisotropic growth process. Due to the preferential absorption

of Cu(I)–Cl^- complex ions on {111} facets, deposition of Cu atoms mainly occurred on the {111} facets and thus led to the anisotropic growth of Cu nanostructures. Apart from Cu(I)–Cl^- complex ions, free Cu(II) and Cu(I) ions in the solution could also be reduced to Cu atoms by OLA. Unlike Cu(I)–Cl^- complex ions, the deposition of Cu atoms generated directly from free Cu(II) and Cu(I) ions is less selective. In reaction systems with Br^- ions or a smaller amount of Cl^- ions, the higher concentrations of free Cu(II) and Cu(I) ions led to an increase in the average diameters of nanowires during the growing process.

Reaction mechanism and the synthesis of Cu nanowires with tunable diameters

Through combining the reaction phenomena and analyses shown above, a reaction mechanism was proposed (Scheme 1). Cu(II) ions were reduced by oleylamine at 165 °C to Cu(I) ions or Cu atoms with the aid of Ni(II) ions. The aggregation and deposition of Cu atoms caused the formation of Cu nanoparticles with diameters around 18 nm. These pre-formed nanoparticles would gradually disappear after the addition of $CuCl_2$ due to the comproportional reaction between Cu(II) ions and Cu. The coordination between Cu(I) ions and X^- further accelerated the etching of pre-formed nanoparticles, and finally led to a clear solution with orange-yellow color. Some pre-formed nanoparticles survived the etching process and nanoseeds formed on the basis of these particles. Anisotropic growth would then occur along the ⟨110⟩ direction due to the preferential absorption of oleylamine and halide ions to form Cu nanowires with few unwanted shapes.

The efforts towards the controllable synthesis of high-quality Cu nanowires with tunable diameters could be achieved through a kinetically controlled synthesis process. Kinetic control could not only effectively tune the size of the nanoseeds, but also influence the growth of one-dimensional nanostructures, which enables the synthesis of Cu nanowires with tunable diameters. The essence of kinetic control is the regulation of the reduction or decomposition rate of a precursor, which could be easily achieved by adjusting the concentration or species of halide ions. Through adjusting the amount and species of halide ions, Cu nanowires with tunable diameters from 20 nm to 90 nm could be successfully synthesized

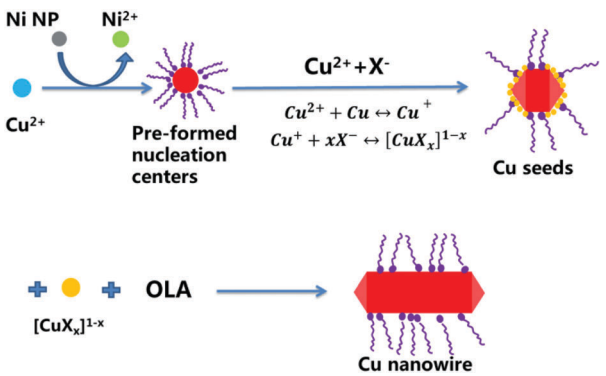

Scheme 1 Schematic illustration of the mechanism of a typical synthesis procedure.

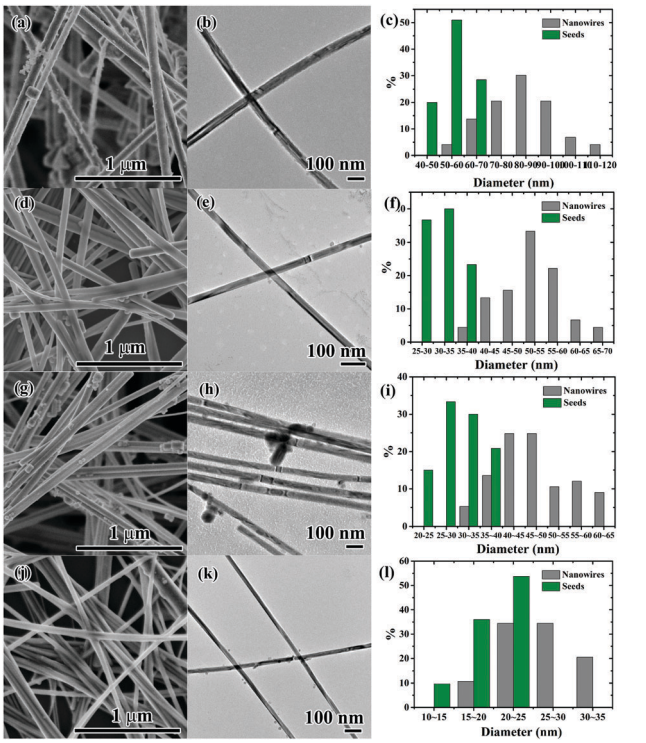

Fig. 4 SEM image (a), TEM image (b) and the diameter distribution (c) of Cu nanowires synthesized with different amounts and species of CuX_2. (a)–(c) 0.8 mmol $CuBr_2$; (d)–(f) 0.8 mmol $CuCl_2$; (g)–(i) 0.8 mmol $CuCl_2$ & 0.2 mmol $NiCl_2$; (j)–(l) 0.8 mmol $CuCl_2$ & 0.5 mmol $NiCl_2$.

(Fig. 4). When 0.8 mmol $CuCl_2$ alone was used in Stage II, Cu nanowires with an average diameter of 62 nm could be obtained (Fig. 4d–f). $NiCl_2$ was added to the solution in order to tune the amount of Cl^- while without changing the concentration of Cu(II) ions. With the amount of $NiCl_2$ increasing from 0.2 mmol (0.8 mmol $CuCl_2$ and 0.2 mmol $NiCl_2$) to 0.5 mmol (0.8 mmol $CuCl_2$ and 0.5 mmol $NiCl_2$), the average diameters of Cu nanowires changed from 47 nm to 20 nm (Fig. 4i and l). Apart from Cl^- ions, Br^- ions were also used to tune the diameter of Cu nanowires.

When 0.8 mmol $CuCl_2$ was replaced by 0.8 mmol $CuBr_2$, the average diameter of Cu nanowires increased from 62 to 90 nm (Fig. 4d and h). As aforementioned, smaller nanoseeds would form when a higher concentration of halide ions was used in the synthesis system. As the anisotropic growth of Cu nanowires occurred on the basis of these nanoseeds, nanowires with smaller diameters would form under this circumstance. Besides, a higher concentration of halide ions could also improve the selectivity of the deposition of Cu atoms during the anisotropic growing process, which could further regulate the diameter of nanowires. The synergistic effects of these two factors result in Cu nanowires with tunable diameters. No Ni was detected in the nanoseeds or the nanowires, confirming that Ni ions did not participate in the growing process of Cu nanowires. The differences between the standard reduction potentials of Cu(I) ions and Ni ions make $NiCl_2$ a great candidate for adjusting the concentration of halide ions.

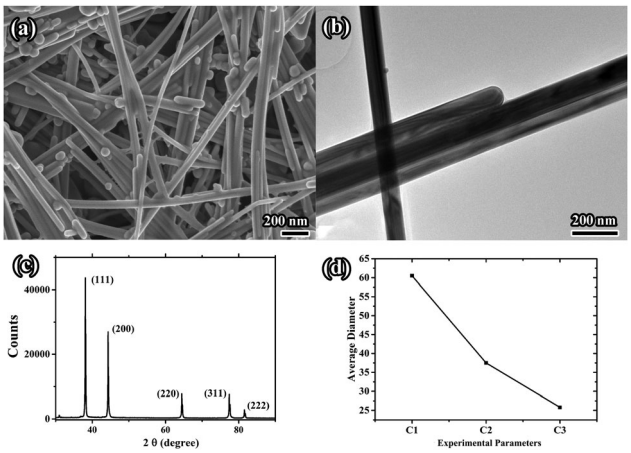

Fig. 5 SEM image (a), TEM image (b), XRD spectrum (c) and the average diameters (d) of Ag nanowires synthesized under different conditions: C1 (1 mmol $AgNO_3$); C2 (0.2 mmol $AgNO_3$ and 0.8 mmol AgBr); C3 (1 mmol AgBr).

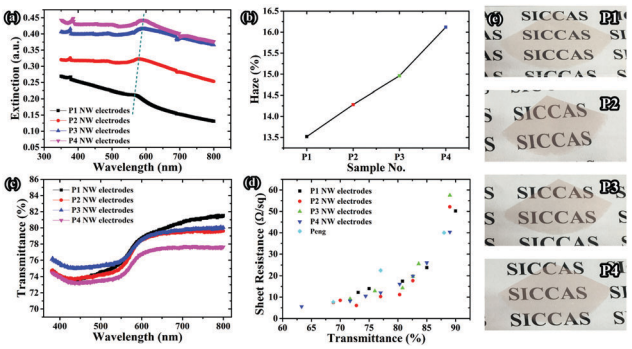

Fig. 6 Extinction spectra (a), optical haze factors (b), transmittance spectra (c), opto-electrical performances (d) and photographs (e) of electrodes composed of Cu nanowires synthesized under different synthesis conditions. P1: 0.8 mmol $CuCl_2$ & 0.5 mmol $NiCl_2$; P2: 0.8 mmol $CuCl_2$ & 0.2 mmol $NiCl_2$; P3: 0.8 mmol $CuCl_2$; P4: 0.8 mmol $CuBr_2$.

Similar to average diameters, the lengths and aspect ratios of nanowires also play an essential role in constructing high-performance devices[12] and vary with the adjustment of reaction parameters (Fig. S6, ESI†). For Cu nanowires with an average diameter of 20 nm, an average length of 17.3 μm and an aspect ratio of 865 could be observed. As the average diameter of Cu nanowires increased from 47 nm to 62 nm and 90 nm, the average length of Cu nanowires increased from 20.9 μm to 25.8 μm and 52 μm and the aspect ratios varied from 445 to 416 and 578. However, the relationship between the concentration of halide ions and the length of nanowires is still unclear.

The ability of controlling over the morphology of Cu nanostructures through adjusting the species and amount of halide ions inspired the controllable synthesis of other metal nanostructures. Ag has a similar lattice structure to Cu.[17] A similar mechanism could be further applied to the controllable synthesis of Ag nanostructures. Ag nanowires with uniform diameters and few concomitant nanoparticles were synthesized through a reaction system similar to the one used above (Fig. 5a and b). The XRD spectrum indicated the pure nature of the as-synthesized Ag nanowires (Fig. 5c). $AgNO_3$ and AgBr are used as the precursors, OLA is used as the reducing agent, 0.07 mmol $CuBr_2$ was used to facilitate the growth of Ag nanowires.[18] Unlike the reaction system for Cu nanostructures, the oxidative etching pair here is composed of Br^- and oxygen. Through tuning the concentration of Br^- ions by adjusting the amount of $AgNO_3$ and AgBr, Ag nanostructures with different diameters could be obtained (Fig. S8, ESI†). Similar to Cu nanowires, as the amount of Br^- ions increases from 0.14 mmol to 1.14 mmol, the average diameter of Ag nanowires decreases from 60 nm to 25 nm, indicating a similar role of the halide ions (Fig. 5d).

The characterization of electrodes composed of Cu nanowires with different diameters

It has been well established that the diameter of nanowires may significantly influence their optical and electrical properties, and thus play an important part in determining the performance of nanowire electrodes. The successful synthesis of high quality Cu nanowires with different diameters enables the experimental characterization of the optical and electrical properties of nanowires and the electrodes based on them (Fig. 6). Peaks near the wavelength of 560 nm were observed when characterizing the UV-vis spectra of Cu nanowires dispersed in ethanol (Fig. 6a). These peaks could be attributed to the excitation of local surface plasmon resonance (LSPR), which is highly sensitive to the material and micromorphology (size, size distribution and shape) of the nanostructures.[19,20] As the average diameter of the Cu nanowires increased from ~20 nm to ~90 nm, the center of the peak changed from 575 to 590 nm. The red shift of LSPR peaks represented a decrease in the restoring force on the oscillating electrons, which was caused by the increment of the diameter of Cu nanowires. Similar results have been found for Ag nanowires with different diameters and Cu nanostructures with different shapes and sizes.[19,21] The characterization of the numerical relationship between the LSPR peak centers and the diameter of Cu nanowires gives us a facial and useful way in analyzing the micromorphology of Cu nanowires. Optical haze is another important optical property that may influence the performances of devices based on Cu nanowire electrodes. The haze factor represents the proportion of the light scattered forward through the electrodes, which could be calculated through analysing the total transmittance and the light scattering rate of the electrodes (eqn (2)):[13,22]

$$\text{Haze} = \frac{\text{forward scattered light}}{\text{forward nonscattered light} + \text{forward scattered light}} \times 100\% = \frac{\text{scatterring rate}}{\text{total transmittance}} \times 100\% \quad (2)$$

Electrodes with higher haze factors could improve the light absorption efficiency in the active layers of solar cells due to the enhanced path length of light.[22] However, nanowire electrodes with a lower haze factor is essential for improving the clarity of display applications.[23] On the basis of Cu nanowires with

different diameters, the optical haze factors of different electrodes were characterized. For electrodes with similar transmittance (~75%), the haze factor increased as the diameter of nanowires increased (Fig. 6b). The results indicated that Cu nanowires with larger diameters might be more suitable for solar cells while Cu nanowires with smaller diameters would be beneficial for display devices.[3] Electrodes composed of nanowires with different diameters exhibited similar transmittance spectra in the visible range (Fig. 6c). Fig. 6d shows the sheet resistance of Cu nanowire electrodes composed of different nanowires as a function of their transmission at a wavelength of 550 nm. All kinds of nanowire electrodes exhibited superior conductivity with a figure of merit (FoM) of around 140 ($T\% \sim 80\%$, $R_s \sim 11\ \Omega\ sq^{-1}$), higher than the ones reported previously (FoM ~ 87).[9] These outstanding electrical performances of Cu nanowire electrodes could be attributed to the uniform distribution of the diameter of the Cu nanowires and the effective elimination of concomitant nanoparticles. Similar FoMs were observed for different electrodes, which could be understood by the balance between the light scattering properties and the conductivity of nanowires. For nanowires with larger diameters, lower resistance was expected due to a weaker boundary scattering effect. However, nanowires with smaller diameters showed higher aspect ratios compared with the nanowires with larger diameters, which was favourable for constructing electrodes with high FoMs. Besides, nanowires with smaller diameters usually exhibit a smaller scattering area, which could benefit the transmittance of nanowire electrodes and further improve the FoMs of nanowire electrodes. The synergetic effect of these factors finally results in electrodes with similar electrical performance. Though having similar conductivity, electrodes composed of Cu nanowires with different diameters may exhibit advantages and disadvantages in different applications. The purposive arrangement of nanowires may show great advantages in the optimization of devices.

Conclusions

In summary, we have proposed a two-step method through which high-quality Cu nanowires with tunable diameters could be synthesized. Kinetically controlled synthesis was achieved by purposively regulating the oxidative etching process, which provides us with a facile and effectively way to accomplish the controllable synthesis of Cu nanowires with few concomitant nanoparticles and uniform diameters. Cu nanowires with various diameters ranging from 20 nm to ~ 90 nm could be achieved through adjusting the amount and species of halide ions. Nanowire electrodes with superior conductivity and high FoMs (FoM ~ 140, 11 $\Omega\ sq^{-1}$@80%,) were constructed on the basis of the high-quality nanowires. The diameter of Cu nanowires was proven to have a great influence on their optical properties. A red shift of the LSPR peak (from 575–590 nm) of the Cu nanowire dispersion and an increment of the haze factors (from 13.5–16.2%, $T\% \sim 75\%$) of the Cu nanowire electrodes were observed. The method could be further applied to the controllable synthesis of Ag nanowires. Ag nanowires with average diameters ranging from 25 to 60 nm were synthesized. As oxidative etching and preferential absorption widely exist in the synthesis of variable metal nanostructures, the method may also be extended to the controllable synthesis of other one-dimensional metal nanostructures or even other nanostructures, which provides a new way for the controllable synthesis of metal nanostructures and the construction of high-performance devices.

Conflicts of interest

There are no conflicts of interest to declare.

Acknowledgements

This work was financially supported by the National Natural Science Foundation of China (Grant No. 61301036), the Youth Innovation Promotion Association CAS (2014226), Shanghai Key Basic Research Project (Grant No. 16JC1402300) and the Major State Research Development Program of China (2016YFA0203000).

Notes and references

1 T. M. Barnes, M. O. Reese, J. D. Bergeson, B. A. Larsen, J. L. Blackburn, M. C. Beard, J. Bult and J. van de Lagemaat, *Adv. Energy Mater.*, 2012, **2**, 353; Z. Chen, A. R. Rathmell, S. Ye, A. R. Wilson and B. J. Wiley, *Angew. Chem., Int. Ed.*, 2013, **52**, 13708; D. S. Hecht, L. Hu and G. Irvin, *Adv. Mater.*, 2011, **23**, 1482; S. Ye, A. R. Rathmell, Z. Chen, I. E. Stewart and B. J. Wiley, *Adv. Mater.*, 2014, **26**, 6670; K. Ellmer, *Nat. Photonics*, 2012, **6**, 809; S. G. Park, C. Mun, M. Lee, T. Y. Jeon, H. S. Shim, Y. J. Lee, J. D. Kwon, C. S. Kim and D. H. Kim, *Adv. Mater.*, 2015, **27**, 4290; Y. Z. Zhang, Y. Wang, T. Cheng, W. Y. Lai, H. Pang and W. Huang, *Chem. Soc. Rev.*, 2015, **44**, 5181; T. Cheng, Y.-Z. Zhang, J.-D. Zhang, W.-Y. Lai and W. Huang, *J. Mater. Chem. A*, 2016, **4**, 10493.

2 D. Zhang, R. Wang, M. Wen, D. Weng, X. Cui, J. Sun, H. Li and Y. Lu, *J. Am. Chem. Soc.*, 2012, **134**, 14283.

3 B. Y. Wang, T. H. Yoo, J. W. Lim, B. I. Sang, D. S. Lim, W. K. Choi, K. Hwang do and Y. J. Oh, *Small*, 2015, **11**, 1905.

4 S. E. H. Murph, C. J. Murphy, A. Leach and K. Gall, *Cryst. Growth Des.*, 2015, **15**, 1968; X. Wang, R. Wang, L. Shi and J. Sun, *Small*, 2015, **11**, 4737; T. Cheng, Y.-Z. Zhang, W.-Y. Lai, Y. Chen, W.-J. Zeng and W. Huang, *J. Mater. Chem. C*, 2014, **2**, 10369; J. Song, J. Li, J. Xu and H. Zeng, *Nano Lett.*, 2014, **14**, 6298; J. Xue, J. Song, Y. Zou, C. Huo, Y. Dong, L. Xu, J. Li and H. Zeng, *RSC Adv.*, 2016, **6**, 91394; J. Xue, J. Song, Y. Dong, L. Xu, J. Li and H. Zeng, *Sci. Bull.*, 2017, **62**, 143.

5 Y. Cheng, R. Wang, J. Sun and L. Gao, *ACS Nano*, 2015, **9**, 3887; P. Lee, J. Lee, H. Lee, J. Yeo, S. Hong, K. H. Nam, D. Lee, S. S. Lee and S. H. Ko, *Adv. Mater.*, 2012, **24**, 3326; T. Cheng, Y. Zhang, W. Y. Lai and W. Huang, *Adv. Mater.*, 2015, **27**, 3349; T. Cheng, Y.-Z. Zhang, J.-P. Yi, L. Yang, J.-D. Zhang, W.-Y. Lai and W. Huang, *J. Mater. Chem. A*, 2016, **4**, 13754.

6 Z. Yu, L. Li, Q. Zhang, W. Hu and Q. Pei, *Adv. Mater.*, 2011, **23**, 4453; X. Wang, R. Wang, H. Zhai, X. Shen, T. Wang, L. Shi, R. Yu and J. Sun, *ACS Appl. Mater. Interfaces*, 2016, **8**, 28831.
7 M. Jin, G. He, H. Zhang, J. Zeng, Z. Xie and Y. Xia, *Angew. Chem.*, 2011, **50**, 10560.
8 Y. Cheng, S. Wang, R. Wang, J. Sun and L. Gao, *J. Mater. Chem. C*, 2014, **2**, 5309.
9 H. Guo, N. Lin, Y. Chen, Z. Wang, Q. Xie, T. Zheng, N. Gao, S. Li, J. Kang, D. Cai and D. L. Peng, *Sci. Rep.*, 2013, **3**, 2323.
10 J. W. Borchert, I. E. Stewart, S. Ye, A. R. Rathmell, B. J. Wiley and K. I. Winey, *Nanoscale*, 2015, **7**, 14496.
11 K. C. Pradel, K. Sohn and J. Huang, *Angew. Chem.*, 2011, **50**, 3412.
12 S. M. Bergin, Y. H. Chen, A. R. Rathmell, P. Charbonneau, Z. Y. Li and B. J. Wiley, *Nanoscale*, 2012, **4**, 1996.
13 F. Cui, Y. Yu, L. Dou, J. Sun, Q. Yang, C. Schildknecht, K. Schierle-Arndt and P. Yang, *Nano Lett.*, 2015, **15**, 7610.
14 Y. Xia, Y. Xiong, B. Lim and S. E. Skrabalak, *Angew. Chem.*, 2009, **48**, 60.
15 R. Long, S. Zhou, B. J. Wiley and Y. Xiong, *Chem. Soc. Rev.*, 2014, **43**, 6288.
16 S. Giuffrida, G. G. Condorelli, L. L. Costanzo, I. L. Fragalà, G. Ventimiglia and G. Vecchio, *Chem. Mater.*, 2004, **16**, 1260.
17 B. Wiley, Y. Sun and Y. Xia, *Acc. Chem. Res.*, 2007, **40**, 1067; B. Wiley, Y. Sun and Y. Xia, *Langmuir*, 2005, **21**, 8077.
18 K. E. Korte, S. E. Skrabalak and Y. Xia, *J. Mater. Chem.*, 2008, **18**, 437.
19 J. van de Groep, P. Spinelli and A. Polman, *Nano Lett.*, 2012, **12**, 3138.
20 E. Hutter and J. H. Fendler, *Adv. Mater.*, 2004, **16**, 1685.
21 H. Guo, Y. Chen, H. Ping, J. Jin and D. L. Peng, *Nanoscale*, 2013, **5**, 2394.
22 C. Preston, Y. Xu, X. Han, J. N. Munday and L. Hu, *Nano Res.*, 2013, **6**, 461.
23 M. M. Menamparambath, K. Yang, H. H. Kim, O. S. Bae, M. S. Jeong, J. Y. Choi and S. Baik, *Nanotechnology*, 2016, **27**, 465706.

